or a real positive pole becomes dominant at

$$\omega_{A_{RPP}} \approx \frac{(g_{M4} + g_0)g_{M2}R_L + (g_{M4} + g_0) - Mg_{M2}}{C_{bs4} + C_{gs2} + C_0} \quad (7)$$

with heavy load resistances R_L. Having the possibility of controlling the gain of the current mirror M, the output impedance of the voltage buffer can be tuned. This can be achieved either by using a tunable current amplifier [3], or in a small range using the regulated cascode current mirror [4] with different regulation currents.

Criterion of stability: Because the output impedance of the CVB is defined by the subtraction of g_ms of transistors (eqn. 2) it can become negative, and that can introduce instability in many applications. To avoid an unstable circuit the gain of the current mirror should fulfil the condition

$$M < \frac{g_{M4} + g_0}{g_{M2}} \quad (8)$$

In this case the pole pair from eqn. (6) of the voltage transfer function cannot move into the right half-plane.

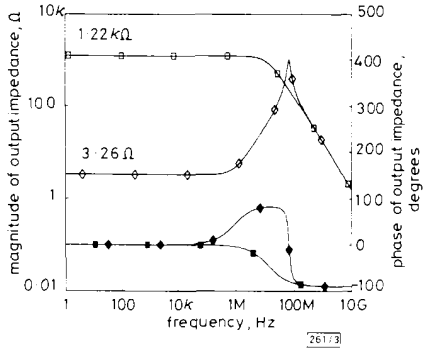

Fig. 3 *Plot of output impedance AC characteristics*
- □ OVB magnitude
- ■ OVB phase
- ◇ CVB magnitude
- ◆ CVB phase

Simulation results: The performance of the circuit with a capacitive load of $C_L = 10\,\text{pF}$ connected to the output was simulated on PSPICE using simplified Level 2 transistor model parameters for a commercially available CMOS process. In Fig. 3 the AC characteristic of the output impedance of the CVB is compared with the output impedance of the OVB having the same transistor sizes. At low frequencies it shows a significant improvement of the output impedance value. At 993 kHz the zero described in eqn. 3 is placed, and at 67·6 MHz the peak given by eqn. 4 can be found. After the peak the output impedance of the CVB follows the output impedance of the OVB. Further, the AC transfer characteristics are shown in Fig. 4. Having a light load at the output the transfer function exhibits a complex conjugate pole pair peak at 66 MHz (eqn. 6), which results in a damped oscillation of the output voltage in response to a step function. The connection of a heavy load at the output leads to the dominance of the first-order pole at 3·72 MHz (eqn. 7).

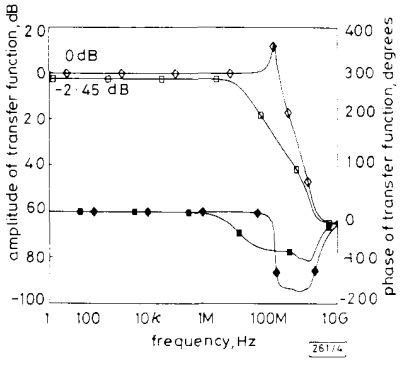

Fig. 4 *Plot of transfer function AC characteristics*
- □ CVB amplitude with $R_L = 100\,\text{k}\Omega$
- ■ CVB phase with $R_L = 100\,\text{k}\Omega$
- ◇ CVB amplitude with $R_L = 10\,\Omega$
- ◆ CVB phase with $R_L = 10\,\Omega$

Conclusions: In this paper a low output impedance CMOS voltage buffer exploiting the compensation technique (CVB) has been introduced. This technique makes it possible to build voltage buffers with low output impedances using small transistor sizes and low bias currents, and an electronic tuning of the output impedance, by choosing a current mirror gain, as well. Further, the compensation technique makes it possible to achieve negative impedances, which can be useful in the design of both grounded and floating negative resistors.

Acknowledgment: This work was carried out with funding from the Danish Research Academy, journal number 5910181.

4th September 1992

I. Mucha (*Electronics Institute, Technical University of Denmark, Building 349, DK-2800 Lyngby, Denmark*)

References

1 BATTERSBY, N., and TOUMAZOU, C.: 'Class AB switched-current memory for analogue sampled-data systems', *Electron. Lett.*, 1991, **27**, pp. 873–875
2 BRUUN, E.: 'A dual current feedback CMOS op amp'. Proc. 10th NORCHIP Seminar, Helsinki, Finland, 1992
3 SURAKAMPONTORN, W., and KUMWACHARA, K.: 'CMOS-based electronically tunable current conveyor', *Electron. Lett.*, 1992, **28**, pp. 1316–1317
4 SÄCKINGER, E., and GUGGENBÜHL, W.: 'A high-swing, high-impedance MOS cascode circuit', *IEEE Solid-State Circuits*, 1990, **25**, pp. 289–298

SIMPLE ANALYTICAL DESCRIPTION OF PERFORMANCE OF *Y*-JUNCTIONS

G. J. M. Krijnen, H. J. W. M. Hoekstra, P. V. Lambeck and T. J. M. A. Popma

Indexing terms: Electro-optics, Optical switching

Simple analytical expressions, describing the performance of the *Y*-junction as a function of only one parameter, the mode conversion factor (MCF), are derived. The expressions are based on numerical studies of *Y*-junctions with varying MCFs by means of the finite-difference beam propagation method (FDBPM). The simple expressions are compared with published switching curves of electro-optic *Y*-junction switches and found to be in excellent agreement.

Introduction: *Y*-junctions are the subject of extensive theoretical and experimental studies [1–5] which are motivated by the versatile applicability (e.g. mode-, power- and polarisation-splitters) and the relaxed fabrication tolerances of these structures. The performance of *Y*-junctions consisting of a bimodal input and two (dissimilar) monomode output branches has been studied theoretically by Burns and Milton [6]. Based on a propagating mode analysis and coupled mode theory they introduced a descriptive parameter for the basic performance of two-dimensional *Y*-junction structures, the so-called mode conversion factor (MCF):

$$MCF = \frac{n_1 - n_2}{\theta\sqrt{[(\bar{n})^2 - (n_b)^2]}} \quad (1)$$

where θ is the tangent of the branching angle α (which is $\approx\alpha$ for small α), n_b is the refractive index of the medium between the two branching arms, $\bar{n} = 0{\cdot}5(n_1 + n_2)$, and n_1 and n_2 are the effective indices of the modes of the branches at infinite separation. Their numerical results showed that diverging Y-junctions, having $|MCF| \gg 0{\cdot}43$, act as mode-splitters, enabling efficient power transfer from each input mode to mainly one of the output channels, whereas $|MCF| < 0{\cdot}43$ leads merely to a division of power over both output channels. Assuming near-adiabatic mode-evolution along the structures it can be expected from reciprocity that in a converging Y-junction with $|MCF| \gg 0{\cdot}43$ a mode launched into one of the input branches will convert selectively to one of the modes of the output, whereas for $|MCF| < 0{\cdot}43$ the power launched into one of the input branches will end up in both output modes. Numerical studies by Yajima [7] confirmed this view. Since then many studies have shown that the MCF has a rather predictive potential.

In this Letter we describe numerical investigations of the performance of Y-junctions with systematically varying MCF values. It is shown that the MCF can be used as the sole parameter in simple analytical expressions, describing the ratio of powers in the two branches of diverging Y-junctions (or the ratio of the powers of both modes of the bimodal section of converging Y-junctions), thereby extending the applicability of the MCF.

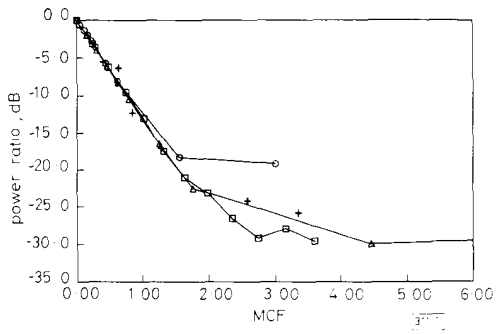

Fig. 1 *Power ratio (in dB) as a function of MCF for series A (□), B (△), C (○) and D (+)*

Simulations: The performance of two-dimensional diverging Y-junctions with largely varying MCF values was examined by means of the scalar finite-difference beam propagation method (FDBPM) [8]. Transverse electric polarised waves were assumed. All structures were chosen to have a bimodal input and two monomode output branches. Four series of Y-junctions, with strongly varying characteristics, were considered (see Table 1). Within each of the series A, B and C, variations in MCF have been introduced by variations in the width of branch 2 only. Series D comprised Y-junctions with variations in index contrast, branching angle and branch widths. The performance of the Y-junctions was characterised by the ratio of the power contained within the channel modes of the branches at sufficient separation. The calculations comprised the cases of launching a TE_0 and a TE_1 mode. Results of the simulations are shown in Fig. 1, where the power ratio is given as a function of the MCF. The results for the case of launching a TE_0 mode are given only since the results for the case of launching a TE_1 mode were virtually identical. Fig. 1 shows that the power ratio, expressed in decibels, is to a good degree a straight line for structures with MCF values up to $\approx 1{\cdot}75$ despite the large variations in geometry and refractive indices. The constant of proportionality of this line, as obtained as the average of the results of all structures with MCF up to 2, is $-12{\cdot}95$ dB. However, for MCF values in excess of 2 the power ratio saturates at values between -20 and -30 dB, the saturation levels depending on the precise geometry of the structure as expected from earlier papers [1, 7]. Moreover, the power ratio of series A shows a slight oscillation with increasing MCF, a feature which was also found experimentally for electro-optical Y-junction switches [3].

Simple expressions: The linear dependence of the power ratio on the MCF, independent of the precise geometry of the Y-junctions, suggests that it can be easily expressed by means of exponential functions. Let P_a denote the output power in system mode A, which is launched at the input, and P_b the power in the other mode. At sufficient separation P_a and P_b will be equal to the power contained in the channel modes of the output branches. Assuming furthermore that negligible input power is converted to radiation modes, the sum of the powers in both output branches equals the input power: $P_a + P_b = P_{in}$. Hence, it follows:

$$P_a = P_{in}\frac{e^{CMCF}}{1 + e^{CMCF}} \tag{2a}$$

$$P_b = P_{in}\frac{1}{1 + e^{CMCF}} \tag{2b}$$

The constant C in the above equations, as determined from the results of the simulations, is 2·98.

Comparison with experimental data: One of the interesting applications of Y-junctions is the electro-optical digital switch [4]. From eqn. 1 it follows that the MCF changes linearly with applied voltage for symmetrical Y-junctions, with opposite voltages applied to the electrodes of both branches. Therefore, to judge the quality of the simple analytic expressions, the predictions of eqn. 2 were compared with published switching curves of electro-optically modulated Y-junction switches. Fig. 2 shows sample points taken from experimental switching curves published in References 3–5, together with the curves as predicted by eqn. 2. To this end the switching curves of the electro-optic Y-junctions, which give the output

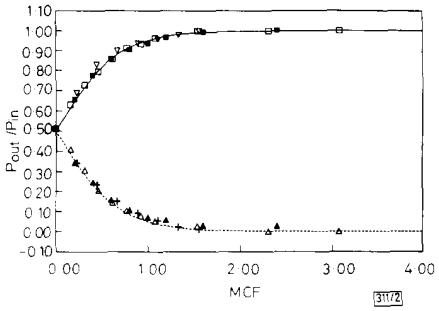

Fig. 2 *Curves as predicted by eqn. 2 and points obtained from experimental electro-optic Y-junction switches as taken from References 3–5*

——— eqn. 2*a*
– – – – eqn. 2*b*
▽+ Reference 3
△□ Reference 4
■▲ Reference 5

Table 1 CHARACTERISTICS OF INVESTIGATED Y-JUNCTIONS

Series	α (deg)	n_s	n_b	W_0	W_1	W_2	λ_0	MCF
				μm	μm	μm	μm	
A	0·10	3·300	3·296	7·50	4·60	2·95–4·60	1·50	0–3·61
B	0·15	1·600	1·595	6·00	5·00	2·00–5·00	1·32	0–8·59
C	0·45	1·600	1·595	6·00	5·00	2·00–5·00	1·32	0–3·00
D	0·5–10	1·600	1·30–1·55	0·80–1·80	0·50–1·20	0·30–1·10	1·32	0·40–12·88

powers as a function of applied voltage, were scaled along the MCF axis. First, it is surprising that the switching curves of the various experimental Y-junction switches have almost similar shapes despite their different geometry and otherwise different technological implementation. This may be a proof that Y-junctions are relatively insensitive to minor technological tolerances. Secondly, the similarity between experimental data and the results of the simple analytic expressions appears to be very good, the difference between them never exceeding a few per cent. These results suggest that eqn. 2 is a good approximation, being helpful for the design of Y-junctions or Y-junction-based switches (such as electro-optical, thermo-optical or opto-optical switches). Moreover, the relation can be used to determine experimentally parameters of electro-optic Y-junction switches, such as electro-optic coefficients or the overlap integrals of electrical and optical fields.

In conclusion, we have shown that Y-junctions can be described by simple analytic formulas, expressing the ratio of the powers in both branches as a function of only one parameter, the mode conversion factor, and yielding accurate results over a range of two orders of magnitude for Y-junctions with MCF values up to 2. The simple expressions are expected to be of great help for the design of Y-junctions and were shown to match accurately the switching characteristics of electro-optic Y-junctions.

9th September 1992

G. J. M. Krijnen, H. J. W. M. Hoekstra, P. V. Lambeck and T. J. M. A. Popma (*Lightwave Devices Group, MESA Institute, University of Twente, PO Box 217, 7500 AE Enschede, The Netherlands*)

References

1 RECOLONS, J., TORNER, L., and CANAL, F.: 'Normalized parameters for Y-branch optical waveguides', *Opt. Lett.*, 1991, **16**, pp. 636–638

2 KRIJNEN, G. J. M.: 'All-optical switching in nonlinear integrated optic devices'. PhD thesis, May 1992, University of Twente

3 OKAYAMA, H., USHIKUBO, T., and KAWAHARA, M.: 'Low-drive-voltage Y-branch digital optical switch', *Electron. Lett.*, 1991, **27**, pp. 24–26

4 SILBERBERG, Y., PERLMUTTER, P., and BARAN, J.: 'Digital optical switch', *Appl. Phys. Lett.*, 1987, **51**, pp. 1230–1232

5 GRANESTRAND, P., LAGERSTRÖM, B., SVENSSON, P., THYLÉN, L., STOLZ, B., BERGVALL, K., FALK, J., and OLOFSSON, H.: 'Integrated optics 4 × 4 switch matrix with digital optical switches', *Electron. Lett.*, 1990, **26**, pp. 4–5

6 BURNS, W., and MILTON, F.: 'Mode conversion in planar dielectric separating waveguides', *IEEE J. Quantum Electron*, 1975, **11**, pp. 32–39

7 YAJIMA, H.: 'Coupled mode analysis of dielectric planar branching waveguides', *IEEE J. Quantum Electron.*, 1978, **14**, pp. 749–755

8 ACCORNERO, R., ARTIGLIA, M., COPPA, G., DI VITA, P., LAPENTA, G., POTENZA, M., and RAVETTO, P.: 'Finite difference methods for the analysis of integrated optical waveguides', *Electron. Lett.*, 1990, **26**, pp. 1959–1960

NETWORK OF 12 OPTICAL SENSORS USING CODE-DIVISION MULTIPLEXING

J. C. Walker, R. Holmes and G. R. Jones

Indexing terms: Optical sensors, Multiplexing, Optical fibres, Spatial light modulators

Spatial light modulators (SLM) have been used recently to multiplex optical sensors. They have a number of advantages that allow a large number of sensors to be networked together with good SNR, low crosstalk levels and without stringent restrictions on the network topology. This letter describes the use of code-division multiplexing (CDM) and reports the results obtained with a 12-sensor network.

Introduction: Time-division multiplexing (TDM) has been successfully implemented using SLM sensor star and matrix networks [1, 2]. A disadvantage of TDM is that light from each sensor in the network is incident on the detector for only a fraction of the duty cycle time; the duty cycle time is the time taken to poll all sensors in the network. This can limit the SNR. An improvement in SNR compared with the TDM system can be achieved by using a CDM scheme which incorporates a pseudorandom bit sequence (PRBS). The technique allows light from each of the sensors to be incident on the detector for just over half the duty cycle, thus permitting the noise bandwidth to be reduced [3]. A PRBS is a finite sequence of bits which appears to be random if the position in the sequence is not known, but if the position in the sequence is known then the bit pattern becomes deterministic [4]. The useful property of a PRBS nominally comprising +1s and −1s bits, is the autocorrelation function which is shown in Fig. 1. It can be seen that the autocorrelation function has a maximum at zero bit shift with an amplitude equal to M (M is the length of the PRBS) and decreases rapidly to a constant level of −1 with a bit shift of one or more bits. It is possible to multiplex a number of signals together by generating a single PRBS and delaying it successively by one bit to produce a series of differentially delayed PRBSs. Each PRBS is modulated independently by a signal which is to be multiplexed and the modulated PRBSs can then be combined. The signals are demultiplexed at the receiver by correlating the multiplexed signal with a reference PRBS which has the same bit shift as the PRBS selected for demultiplexing.

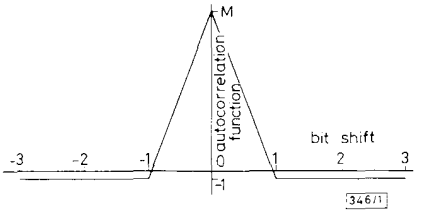

Fig. 1 *Autocorrelation of PRBS*

The nonselected signals are suppressed by a factor $1/M$, and so the crosstalk level is given by $(N\text{-}1)/M$, where N is the number of multiplexed signals. The crosstalk level increases with increasing number of sensors and decreases with increasing length of the PRBS. For a 12-sensor network a PRBS length of 65535 bits would be required to achieve a crosstalk level of better than −70 dB. PRBSs have been used in the past to multiplex three sensors [5] by transmitting a single PRBS of length 255 bits into a ladder network with the propagation delay between sensors being greater than one bit period. The measured signal suppression ratio was 26 dB, while the calculated value was 48 dB. The signal suppression ratio is the ratio of the signal amplitude when correlated to the value when uncorrelated. An estimated crosstalk level for a three-sensor network would be −20 dB. A novel and simple signal processing method has been developed which uses a modified PRBS, that theoretically produces no crosstalk regardless of the length of code used. The modified PRBS comprises +2s and 0s bits and is crosscorrelated with a PRBS which has an idential bit pattern and length but comprises bits with values of +1 and −1. The crosscorrelation function result is shown in Fig. 2, and it can be seen that using this processing method the value of the function at zero bit shift is approximately the same as that obtained with the previous autocorrelation technique. However, once the bit shift becomes greater than 1 bit the function value is zero, which means there is no crosstalk between bit-shifted PRBSs. The modified PRBS is chosen to have nominal bit values of +2 and 0 in order that it has the same AC power as the unmodified PRBS; this allows a fair

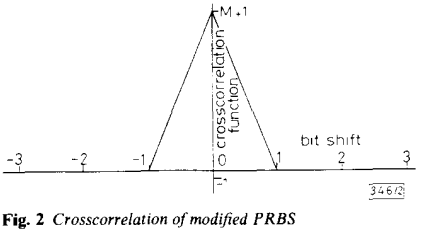

Fig. 2 *Crosscorrelation of modified PRBS*